Discrimination of the Roles of Crosslinking Density and Morphology in the Swelling Behavior of Crosslinked Polymers: Poly(*N*-vinylimidazole) Hydrogels

Isabel E. Pacios, Inés F. Piérola

Department of Ciencias y Técnicas Fisicoquímicas, Universidad a Distancia (UNED), 28040 Madrid, Spain

Received 11 January 2008; accepted 3 October 2008
DOI 10.1002/app.29307
Published online 9 February 2009 in Wiley InterScience (www.interscience.wiley.com).

ABSTRACT: The degree of swelling (*S*) of crosslinked polymers depends on several variables whose individual contributions are difficult to be distinguished. The aim of this work is to determine the contributions of the morphology to *S*, discriminating them from the effect of the crosslinking density. Under usual conditions of synthesis, these two characteristics vary simultaneously but here, several samples of chemically crosslinked poly(*N*-vinylimidazole) having the same permanent crosslinking density (determined by DSC) and different porous morphologies (determined by SEM) were prepared. It was thus found that the variation of *S* with porosity, keeping constant the rest of variables, is strongly solvent dependent. Swelling in methanol is almost constant whereas for ethanol, deionized water, and aqueous HCl solutions, *S* depends on morphological features in a different way for each medium. It was concluded that *S* increases with inherent porosity and solvent effects arise from the counterbalance of such increment with the dependence of the polymer-solvent interaction parameter on the polymer volume fraction. © 2009 Wiley Periodicals, Inc. J Appl Polym Sci 112: 1579–1586, 2009

Key words: poly(*N*-vinylimidazole); hydrogels; crosslinking density; porosity; swelling

INTRODUCTION

Numerous studies published nowadays, focus on a particular type of crosslinked polymers: the hydrogels. The most relevant properties of crosslinked polymers (e.g., swelling, elastic modulus, or permeability) depend on the crosslinking density, the type of crosslinker and the polymer network structure.[1,2] Polymer morphology is also known to have an important incidence on the hydrogel properties.[3–7]

Crosslinked polymers may show pores with quite different size (from nanometer to millimeter diameters), structure (closed or interconnected) and shape (fibrillar networks, honeycomb-like, spherical, cylindrical, channel-like).[3] The porous morphology depends on several variables such as the porogen and crosslinker used in feed, or the previous thermal history of the sample.[3–12] Sponges and macroporous polymers are prepared with porogen agents[9,10] or other porogenic methods.[4,11,13,14] Polymer networks synthesized without using porogens, exhibit pores (inherent porosity[12]) that in the swollen state are filled with solvent and contribute significantly to the degree of swelling.[5,8,11,12]

The roles of morphology and crosslinking in determining polymer properties are difficult to be distinguished because upon changing crosslinking, the morphology changes too.[6,7] Under usual conditions of synthesis, morphology and crosslinking vary simultaneously. In this work, we intend to isolate those two effects and with that purpose we have synthesized a set of samples of chemically crosslinked poly(*N*-vinylimidazole) (PVI) with the same crosslinking density and different morphology.

The crosslinking density experimentally determined is the result of contributions from permanent or covalent crosslinks, network defects and specific topologies of the system and the relative weight of such contributions depends on the technique employed. The physical meaning of the crosslinking density determined with any technique can be discussed by comparison with the values predicted by theoretical models. Tanaka's group proposed a polymer network model showing a single type of network defect: unreacted pendant vinyl groups.[15] According to this model, the crosslinking density (ν_e) is proportional to the total comonomer concentration (C_T) and to the crosslinker concentration employed in the polymerization feed mixture (c_{xl}) in such a way that $\nu_e \approx c_{xl} \times C_T$. With regard to C_T, this dependency is the inverse of the stoichiometric

Correspondence to: I. F. Piérola (ipierola@ccia.uned.es).
Contract grant sponsor: DGI (Spain); contract grant number: CTQ2007-61007/BQU.

TABLE I
Concentration of Crosslinker ([BA]) and Bifunctional Comonomer ([VI]) Employed in the Synthesis of Linear and Crosslinked PVI Samples

Sample code	[VI] (mol/L)	[BA] (mol/L)	$C_T \times$ [BA] $(mol/L)^2$	Y (%)	T_g (°C)	ΔC_p [J/(g K)]
PVI-*l*	4.59	0	0	87.2	179.1	0.32
PVI-6.0	5.95	0.0382	0.229	95.4	185.2	0.34
PVI-5.4	5.34	0.0446	0.240	97.4	185.7	0.34
PVI-4.6	4.52	0.0523	0.239	98.5	185.4	0.31
PVI-4.5	4.43	0.0545	0.245	100	186.0	0.32
PVI-3.9	3.85	0.0605	0.237	100	185.0	0.29
PVI-3.4	3.29	0.0710	0.239	96.2	184.2	0.25
PVI-2.8	2.75	0.0849	0.241	87.8	184.1	0.21
PVI-2.3	2.18	0.1046	0.239	100	183.9	0.18
PVI-1.8	1.64	0.1362	0.242	94.6	185.6	0.16

The yield of the polymerization (Y) and the glass transition temperature (T_g) and the heat capacity jump of the glass transition (ΔC_p) are also shown.

dependency expected for an ideal network without any type of defect: $\nu_e \approx c_{xl}/C_T$. The experimental results of hydrogel samples obtained at almost total conversion, support the prediction of the model by Tanaka, which means that some vinyl groups of the crosslinker remain unreacted, even after total incorporation of the monomers to the polymer network.[11,15–17]

The PVI samples employed in this work were synthesized with C_T and c_{xl} values varying in a broad range, with the constraint that their product is the same for any sample. In this way, their crosslinking density is expected to be the same. However, its morphology is totally different, because it does not depend on $c_{xl} \times C_T$ but on c_{xl}. The crosslinking density and the inherent porosity change significantly throughout postgel reactions[12,17] and only total conversion samples have the predetermined characteristics.

The homopolymers and copolymers of *N*-vinylimidazole are pH sensitive systems[18–21] because imidazole moieties are weak basic groups that become protonated in acid solutions. Protonation converts neutral polymers in polyelectrolytes showing particularly interesting effects[22–25] in which the roles of morphology and crosslinking are imbricated. In this work, both neutral and protonated PVI hydrogels were studied.

EXPERIMENTAL

Materials and synthesis

Poly(*N*-vinylimidazole) hydrogel samples (PVI) were synthesized by radical crosslinking copolymerization of *N*-vinylimidazole (VI), fluorescein-methacrylate (FlMA) and *N,N′*-methylene-bis-acrylamide (BA) in aqueous solution, with 2,2′-azo-bis-isobutyronitrile (AIBN) ($1.03 \times 10^{-2}M$) as initiator. *N*-vinylimidazole (Aldrich, Steinheim, Germany) was distilled under reduced pressure, immediately prior to use. Water was distilled and deionized by a Milli-Q system from Millipore and AIBN (Fluka, Steinheim, Germany) was recrystallized from methanol. BA (Aldrich) and FlMA (Aldrich) were high quality products used as received. FlMA concentration was $1.5 \times 10^{-5}M$ in all cases whereas the concentration of VI and BA in the feed varied for each sample (see Table I) with total comonomer concentrations, C_T, ranging from 1.8 to 6.1M and BA concentration ([BA]) from 0.14 to 0.04M in such a way that their product $C_T \times$ [BA] is approximately constant at 0.239 ± 0.004. Henceforth, hydrogel samples will be denoted as PVI-C_T and the corresponding [BA] can be determined as $0.239/C_T$.

The feed mixtures were poured into glass tubes with 12.8-mm internal diameter. Afterwards, they were sonicated for 15 min, bubbled with argon for 10 min and introduced in a thermostatic bath at 70°C for 44 h. Ten minutes after being introduced in the bath, the tubes were inverted to check movement of their contents, and in all cases, it was found that samples did not flow, indicating that gelation had already taken place. After synthesis, the hydrogel cylinders were taken out of molds; 1-cm thick sample from the top and another from the bottom were ruled out and the central part was cut into disk-like pieces of 12.8-mm diameter (the internal diameter of tubes employed in the synthesis) and less than 1-mm thick.

Linear or uncrosslinked poly(*N*-vinylimidazole) (PVI-*l*) was synthesized in aqueous solution, at 70°C, with [VI] = 4.59M and [AIBN] = $1.7 \times 10^{-3}M$ and afterwards it was precipitated over acetone and dried at 70°C for 5 days.

Swelling measurements

For swelling measurements in methanol (MeOH), ethanol (EtOH), and deionized water, samples were

immersed in the swelling solvent immediately following polymerization (without previous drying). During the next 10 days, the bath was frequently changed. From time to time, samples were removed from the bath, blotted with tissue paper and weighed. Once the samples had reached a constant weight (m_h), they were dried slowly in air for 40 days and under vacuum, at room temperature, throughout 10 more days. The weight of xerogels (m_o) was then determined.

Before swelling measurements in HCl aqueous solutions, samples were washed exhaustively in deionized water and dried. Xerogel specimens of known mass (m_o) were immersed in a volume (V) of HCl aqueous solutions of known initial pH_i, required to have in each case the same effective polymer concentration

$$C_{\text{ef}} = \frac{m_o}{M_o V} \tag{1a}$$

where M_o represents the molecular weight of the monomeric unit. The effective polymer concentration is not a real concentration, since the polymer is not dissolved but simply immersed. In this work, C_{ef} was within the range 10.5 ± 1 mM. One month later, samples were weighed (m_h) and the equilibrium pH of the baths (pH_{eq}) were measured. The swelling solution was not replaced to avoid artifacts due to changes of pH. pH measurements were carried out with a Corning 245 pH meter, at room temperature and the degree of protonation (α) was determined as

$$\alpha = \frac{[H^+]_i - [H^+]_{\text{eq}}}{C_{\text{ef}}} \tag{1b}$$

where $[H^+]_i$ and $[H^+]_{\text{eq}}$ represent the initial proton concentration in the swelling medium (before gel immersion) and the concentration at swelling equilibrium, also measured in the swelling bath. Proton concentrations were assumed to be equal to proton activities and were determined from pH measurements in the bath.

The equilibrium degree of swelling, S, was determined as the ratio of the weight of swelling solvent ($m_h - m_o$), to the weight of dry gel: $S = (m_h - m_o)/m_o$. The polymer volume fraction in the equilibrium swollen state, v_2, was determined as

$$v_2 = (1 + \rho_2 S/\rho_1)^{-1} \tag{2}$$

where ρ_2 and ρ_1 represent the density of the dry gel and the swelling medium, respectively. Xerogel densities were pycnometrically determined with acetone, a precipitant of PVI, and it was concluded that they were approximately the same for all the samples, $\rho_2 = 1.225$ g/mL.

An important magnitude in the swelling analysis is v_{2r}, the polymer volume fraction in the relaxed network state, i.e., when the cross-linkages were introduced. It is also called memory parameter. To determine its value, an aliquot of any sample was weighed following polymerization (m_{hr}) and then it was washed and dried. The degree of swelling in the relaxed state was determined as $S_r = (m_{\text{hr}} - m_o)/m_o$ and $v_{2\text{r}}$ was calculated with eq. (2). The yield of the polymerization is

$$Y = 100 v_{2r}/(C_T \times V_2) \tag{3}$$

with V_2 being the molar volume of the polymer in L/mol. Almost total conversion was achieved for all the samples studied (Table I). For a given sample, $v_{2\text{r}}$ is proportional to C_T.

Calorimetric measurements

DSC experiments were carried out by means of a Mettler Toledo 12E calorimeter provided with a DSC822 oven and a subambient cooling unit. Polymer specimens of about 8 mg, determined within ± 0.02 mg by means of a Mettler Toledo AG285 electrobalance, were employed. Two runs were performed with each specimen, in a nitrogen atmosphere, using an empty aluminum cell as a reference. Samples were heated at 90°C for 10 min and first run was then scanned at 5°C/min from 90 to 240°C, a temperature well below the beginning of thermal instability of PVI xerogels.[19,25] A fast cooling at 40°C/min followed it, and second run was scanned at 10°C/min in the range 30–300°C. Only second run results are presented.

As a control, in some cases, the second run was extended only to 240°C and then, the sample was weighed again to determine the loss of water during heating. It was thus found that mass loss was, at most, 10 % and that was the incertitude assigned to the increment in the heat capacity of the glass transition, ΔC_p. Among the several criteria proposed for the determination of T_g, we have taken the inflection point provided by the software of the instrument. At least two experiments with different specimens were performed for each sample and average values are given in Table I. Glass transition temperatures from independent thermograms were reproducible within 1°C. Mean values of ΔC_p were within 10 % of any single value from two or three independent experiments.

SEM measurements

Scanning electron microscopy (SEM) measurements were carried out in a JEOL JSM 6400 electron microscope. The gel samples swollen at equilibrium in deionized water were freeze-dried (Heto CT/DW60E) and coated with gold (Balzers SCD 004

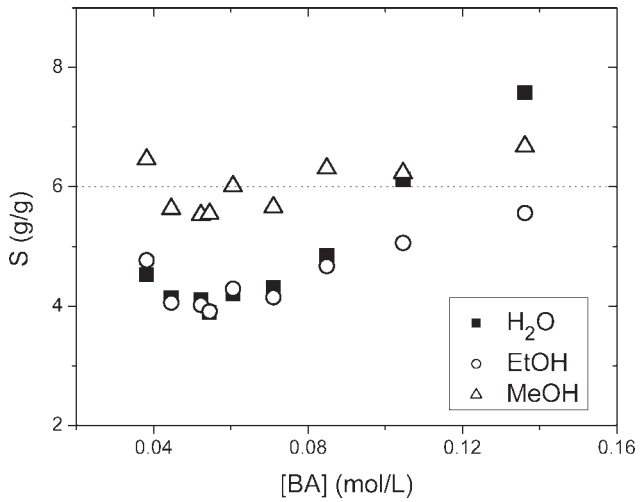

Figure 1 Swelling degree of PVI in deionized water, methanol, and ethanol, at room temperature, plotted as a function of the crosslinker concentration in the feed.

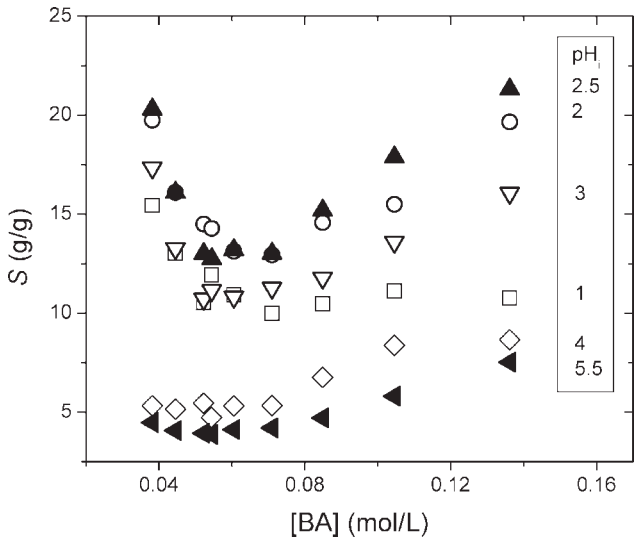

Figure 2 Swelling degree of PVI immersed in HCl aqueous solutions of different initial pH indicated in the insert. Polymer effective concentration $1.0 \times 10^{-2}M$.

sputter-coater). Surface and bulk structures were observed. Inner parts of the specimens were revealed by simply cutting them with a bistoury or by cryogenic fracture. Several specimens of each sample were studied.

RESULTS AND DISCUSSION

PVI hydrogel samples were synthesized with different concentrations of VI and BA (Table I) such that the product $C_T \times$ [BA] is approximately constant at 0.239 ± 0.004. The synthetic conditions were forced (44 h at 70°C) to achieve almost total conversion (Table I) and therefore, all the samples are expected to have the same crosslinking density. Immediately after polymerization some hydrogels are transparent, flexible and compact (those synthesized with the larger C_T), whereas others are opaque and softer (those with larger [BA]). The different optical aspect reveals that the morphology is different.

Figures 1 and 2 show the equilibrium degree of swelling of PVI in several media: organic solvents as MeOH and EtOH, deionized water and HCl aqueous solutions of different pH_i. Constant S or a monotonic increment with [BA] is expected for the samples here employed, on the basis of constant ν_e and v_{2r} proportional to C_T (see below). However, that is not observed for all the swelling media here studied. To understand the swelling behavior it is necessary to separate the contributions of the crosslinking density and the morphology first.

Morphology

SEM micrographs shown in Figure 3 demonstrate that in the swollen state (reproduced in freeze dried samples[11,12]) PVI exhibit pores with different structure and size, depending on feed composition. As no porogen was added to the feed, such porosity is inherent to the polymer morphology in the swollen state.[12]

Micrographs A and C illustrate the two limit cases. Samples synthesized with the largest C_T and

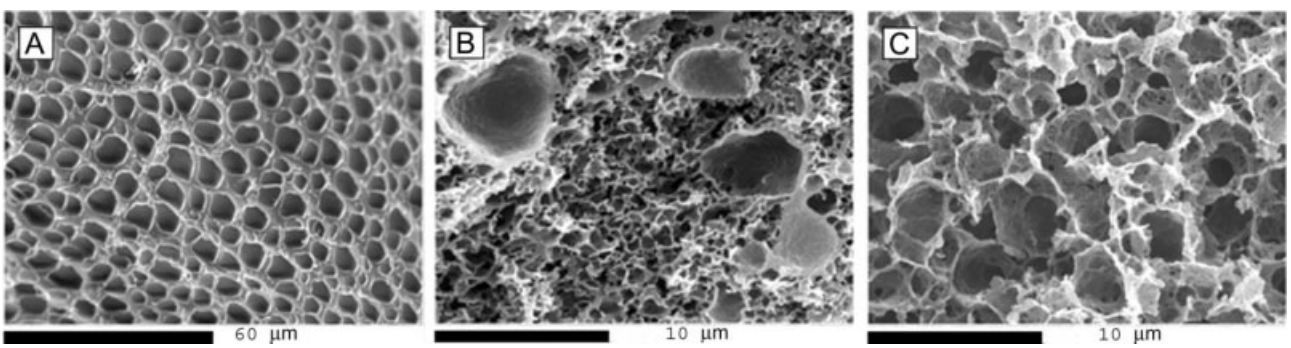

Figure 3 SEM micrographs representative of the morphology of PVI samples synthesized with the following feed conditions: (A) $C_T = 6.1M$, [BA] = $0.039M$; (B) $C_T = 2.8M$, [BA] = $0.086M$; (C) $C_T = 1.8M$, [BA] = $0.137M$.

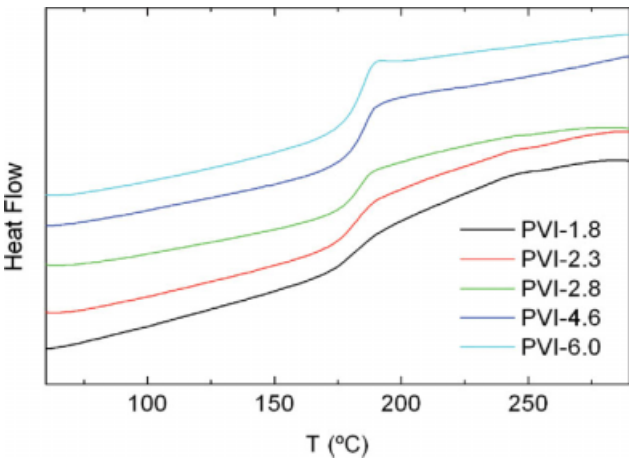

Figure 4 Second run DSC profiles of PVI-C_T samples. [Color figure can be viewed in the online issue, which is available at www.interscience.wiley.com]

lowest [BA] [Fig. 3(A)] show macropores that are large (about 8-μm diameter), spherical and totally closed by thick walls. Thick walls were associated to large C_T for similar systems.[4] In the limit of low C_T and large [BA] [Fig. 3(C)] the macropores are smaller (about 3-μm diameter) but the most significant difference is that they are not completely closed, their walls are thin and incomplete allowing interconnection of all them. For intermediate feed compositions, the two types of macropores are observed, as shown in Figure 3(B).

Nitrogen physisorption measurements demonstrate[12] that for intermediate feed compositions, the total volume of pores is minimum (0.012 cm^3/g vs. 0.066 cm^3/g for PVI-6.1 and 0.052 cm^3/g for PVI-1.8) and corresponds mostly to mesopores (2–50 nm in diameter). For the two limit compositions, both mesopores and macropores (above 50 nm) were observed and the contribution of micropores (below 2 nm) was, in all cases, negligible.[12] The pore size distributions of samples with limit compositions are rather unimodal whereas those of samples with intermediate compositions are multimodal and broader.[12]

Permanent crosslinking density

DSC profiles of PVI xerogels show the pattern depicted in Figure 4: a glass transition whose T_g does not change much and whose heat capacity jump (ΔC_P) depend significantly on the feed composition employed for each sample (Table I). Samples synthesized with the largest [BA] (lowest C_T) show a much broader transition and smaller ΔC_P.

The broadness of the transition is typical[26,27] of crosslinked polymers made by free radical polymerization and corresponds to the heterogeneous distribution of crosslinks in the network. The knots hinder the mobility and the domains with different degree of crosslinking show different T_g's, too close to be resolved in separated transitions. Different types of domains with rigidity within a range limited by that of linear PVI and highly cross-linked poly(*N*,*N*′-methylene-bis-acrylamide) (PBA), coexist in PVI xerogels.[17] ΔC_P is approximately zero for densely crosslinked networks as PBA[17] and therefore, the descent of ΔC_P of samples with large [BA] reveals the existence of increasing portions of PBA-like domains.

In the framework of the Gibbs-DiMarzio theory of glass transitions, the following expression was derived[28] for crosslinked polymers

$$T_g - T_g^L = T_g^L \frac{kM_o\nu_e/\rho_2\gamma}{1 - kM_o\nu_e/\rho_2\gamma} \quad (4)$$

where T_g^L is the glass transition temperature of the uncrosslinked polymer (here 452.2 K); k is a fitting parameter equal to 1.2×10^{-23} in molecular units, for polystyrene and similar polymers; ν_e is the permanent crosslinking density or number of elastic polymer chains, per unit volume of xerogel; and γ is the number of flexible bonds per monomeric unit (2 for polystyrene and similar polymers as PVI). Figure 5 shows $\nu_e(T_g)$, the permanent crosslinking density determined through T_g measurements and eq. (4), and compares it with other approaches to ν_e.

Effective crosslinking density

For neutral hydrogels swollen at equilibrium, the polymer-solvent mixing contribution to the osmotic

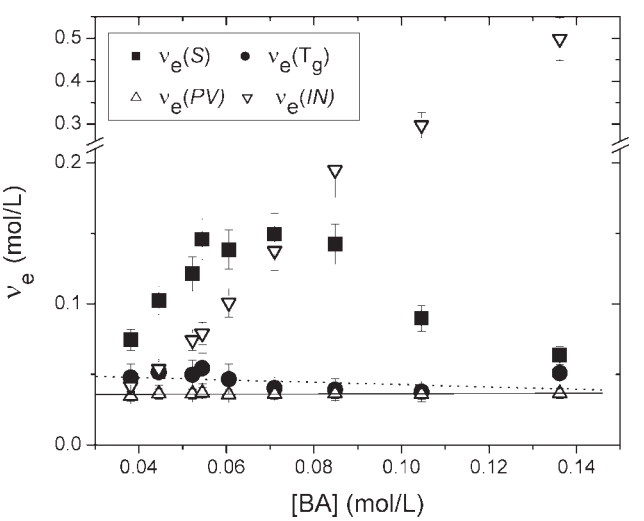

Figure 5 Crosslinking density of PVI samples described in Table I, determined by means of swelling in deionized water, $\nu_e(S)$, and T_g measurements, $\nu_e(T_g)$. Calculated values for ideal stoichiometric polymer networks, ν_e(IN), and for polymer networks with pendant vinyl groups, ν_e(PV), are also plotted.

swelling pressure (Π_{mix}) balance with the elastic contribution (Π_{el}). The Flory-Rehner equation,[29] modified to take into account v_{2r}, the polymer volume fraction immediately after polymerization,[30] expresses such balance ($\Pi_{mix} = -\Pi_{el}$) and relates v_2 with ν_e, the effective crosslinking density:[22,24]

$$\ln(1 - v_2) + v_2 + \chi v_2^2 + V_1 \nu_e (v_{2r}^{2/3} v_2^{1/3} - 2v_2/\phi) = 0 \quad (5)$$

where V_1 represents the solvent molar volume, χ is the polymer-solvent interaction parameter and ϕ the knots functionality ($\phi = 4$ for BA). The affine model and gaussian chains were considered for Π_{el}.[22,24,31] Equation (5), with[16] $\chi = 0.496 + 0.308 v_2$, affords the $\nu_e(S)$ values plotted in Figure 5 for PVI swollen in deionized water.

Physical meaning of permanent and effective crosslinking densities

It was previously shown[11,15–17] that, in accordance with the model of polymer network with pendant vinyl groups proposed by Tanaka,[15] all the samples synthesized with the same $C_T \times$ [BA] have the same crosslinking density

$$\nu_e(\mathrm{PV}) = a^6 C_T [\mathrm{BA}] \rho_2 / M_o \quad (6)$$

where a^6 equals the product of the molar volumes of bifunctional monomer and crosslinker (0.01158 L^2/mol^2 for PVI crosslinked with BA).[16,17] These ν_e(PV) values are also depicted in Figure 5 together with ν_e(IN), the stoichiometric crosslinking density of an ideal polymer network without defects

$$\nu_e(\mathrm{IN}) = [\mathrm{BA}] \rho_2 / 2 C_T M_o \quad (7)$$

Error bars for $\nu_e(T_g)$ in Figure 5 correspond to 20% and come from about 1.4°C incertitude in the difference $T_g - T_g^L \cong 7$°C (see Table I). The error bars for the other magnitudes correspond to 10% uncertainty.

Figure 5 shows how in the limit of low [BA], both $\nu_e(T_g)$ and $\nu_e(S)$ tend to the model values ν_e(PV) and ν_e(IN), which are almost coincident in that plot side. However, in the other side, both $\nu_e(T_g)$ and $\nu_e(S)$ are much smaller than ν_e(IN), thereby indicating that a large proportion of crosslinker molecules are involved in network defects, which in principle can be dangling chains, large sequences of crosslinker, pendant vinyl groups or intramolecular cycles. For PVI, the existence of pendant vinyl groups accounts for the observed $\nu_e(T_g)$, since it shows an excellent coincidence with ν_e(PV) and both are almost constant. This means that, in the solid state, the pores collapse and the topological details disappear in such a way that $\nu_e(T_g)$ measures something in common to all the samples, that is, covalent or permanent junctions of the primary or molecular polymer network.

Nevertheless, morphological features are included in the effective crosslinking density $\nu_e(S)$, which is measured in the swollen state, unlike $\nu_e(T_g)$. The inherent porosity diminishes $\nu_e(S)$, because solvent retained in voids behaves as external water rather than as water swelling the primary polymer network[11,12] and yields apparent v_2 values smaller than for the hypothetical non-porous network. In this way, the habit of $\nu_e(S)$ versus [BA] is the same as for the inverse of the porosity, showing a maximum at the compositions of minimum porosity. The determination of the crosslinking density through swelling measurements was recently questioned for these and other reasons.[12,31] What we conclude is that it must be understood, not as the crosslinking density of the molecular polymer network, but as an effective value that reflects crosslinking points and inherent porosity.

Solvent effects

On the basis of constant ν_e and v_{2r} proportional to C_T, eq. (5) predicts a monotonic descent of v_2 (i.e., an increment of S) with increasing [BA]. The influence of v_{2r} is numerically less significant with regard to that of ν_e. Consequently, samples described in Table I, are expected to have similar S in a given solvent, even though they correspond to different C_T and therefore different v_{2r} [see eq. (3)]. Figures 1 and 2 show that it is not the observed behavior, which is solvent dependent.

In MeOH (Fig. 1), S scarcely changes with [BA] (or alternatively with C_T) but in deionized water and in ethanol, S is minimum for intermediate values of [BA]. In aqueous HCl solutions of different pH_i (Fig. 2), S depends significantly on [BA]. In this last plot, it may be observed that, for each sample, S increases upon decreasing pH_i due to partial protonation of the basic imidazole rings. Protonation gives place to an ionic osmotic swelling pressure that increases solvent uptake.[18,19,24] Above a certain degree of protonation equivalent to the critical charge density of Manning, the counterions condensate and the ionic contribution decreases[18] in concordance with the descent of swelling at pH_i below 2.5, observed in Figure 2. It is remarkable in that plot that some curves are more symmetric than others with respect to the minimum, indicating that two independent morphological features operate in the two limits of composition, the lowest or largest [BA]. This suggests that closed (lowest [BA]) and interconnected pores (largest [BA]) have a different incidence on swelling.

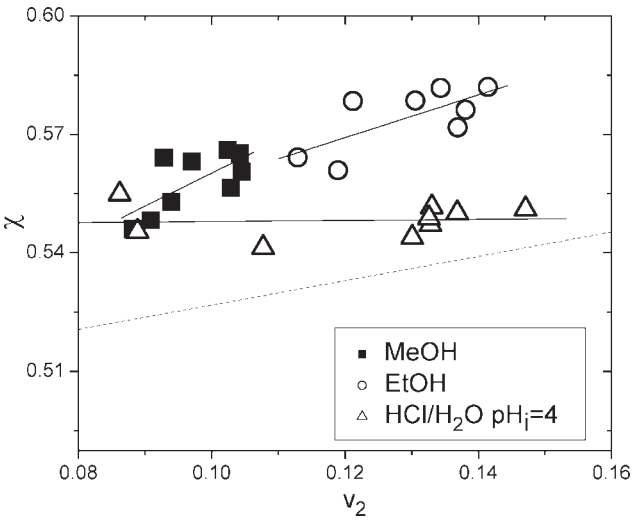

Figure 6 Polymer-solvent interaction parameter of PVI samples (Table I) swollen in methanol, ethanol and HCl aqueous solution with $pH_i = 4$. The dashed line represents the interaction parameter of PVI-deionized water.

Swelling depends on solvent through χ and V_1. Once $\nu_e(S)$ was determined (from S data in water), χ for ethanol and methanol may be obtained, through eq. (5), as a function of v_2, as shown in Figure 6. The polymer-solvent interaction parameter is greater in gels than in dilute solutions of the corresponding soluble polymer and it seems to be well represented[31,32] by a linear function of the polymer volume fraction in the swollen network: $\chi = \chi_1 + \chi_2 v_2$, that follows from quasi chemical equilibrium theory.[33] It was recently emphasized the importance of taking into account the concentration dependence of χ in the correct analysis of swelling data.[31–33] Unfortunately, there are only a few number of results reported on this topic.

Figure 6 shows the best-fit lines corresponding to $\chi = (0.48 \pm 0.03) + (0.8 \pm 0.3)v_2$ for PVI-methanol and $\chi = (0.50 \pm 0.03) + (0.5 \pm 0.2)v_2$ for PVI-ethanol. To obtain χ in acid solutions, the protonation of the imidazole rings and the subsequent ionic contribution to the osmotic swelling pressure must be considered[22,24] and thus, it results that $\chi = (0.547 \pm 0.008) + (0.01 \pm 0.07)v_2$, for PVI swollen in HCl aqueous solution with $pH_i = 4$, which corresponds to a degree of protonation within the range 0.0121 ± 0.0005.

It is remarkable in Figure 6 that the larger is the dependence of χ on v_2, i.e., the larger is χ_2, the smaller is the dependence of S on [BA]. Thus, for methanol, χ shows the largest slope and swelling is practically independent on feed composition (Fig. 1). In Contrast, swelling in HCl aqueous solution is clearly dependent on feed (Fig. 2), and the corresponding χ yield the smallest slope.

It seems that changes of χ with v_2 counterbalance with changes of v_{2r} and morphological changes included in $\nu_e(S)$. Total compensation of both effects requires large slopes of χ with v_2, as accomplished for methanol but not for the other swelling media.

CONCLUSIONS

Swelling depends on polymer morphology, crosslinking density, memory parameter, and polymer-solvent interaction parameter. By its side, morphology, crosslinking density, and memory parameter depend on feed compositions and are closely interrelated. Trying to discern between the roles of morphology and crosslinking density, we have analyzed the swelling behavior of a set of PVI samples in several media. They were synthesized in conditions such that C_T and [BA] were different for each sample but $C_T \times$ [BA] was the same for all them. As expected from predictions of the model by Tanaka's group, all these samples have almost the same permanent crosslinking density $\nu_e(T_g)$. However, they show different morphology. Morphological features are included in the effective crosslinking density $\nu_e(S)$, which is proportional to the inverse of the porosity of freeze-dried samples. In this way, it can be considered that $\nu_e(S)$ and $\nu_e(T_g)$ represent the separated roles of morphology and permanent crosslinking density, respectively.

Regarding the solvent effect, the different swelling behavior in different media was explained by the dependence of χ on the polymer concentration in the swollen network: $\chi = \chi_1 + \chi_2 v_2$. If such dependence is large, as in methanol, it compensates the variation of v_{2r} and $\nu_e(S)$ with feed composition and thus, S is almost constant. Solvents with small χ_2 show more pronouncedly the influence of inherent porosity through $\nu_e(S)$ and have S values highly dependent on feed composition.

SEM measurements were carried out in the Centro de Microscopía Electrónica "Luis Bru" of the Universidad Complutense.

References

1. Geissler, E., Ed. Functional Networks and Gels; Wiley-VCH: Weinheim, Germany, 2003.
2. Xue, W.; Champ, S.; Huglin, M. B. Polymer 2001, 42, 3665.
3. Pacios, I. E.; Pastoriza, A.; Pierola, I. F. Colloid Polym Sci 2006, 285, 263.
4. Dinu, M. V.; Ozmen, M. M.; Dragan, E. S.; Okay, O. Polymer 2007, 48, 195.
5. Turan, E.; Caykara, T. J Appl Polym Sci 2007, 106, 2000.
6. Aroca, A. S.; Fernández, A. J. C.; Ribelles, J. L. G.; Pradas, M. M.; Ferrer, G.; Pissis, P. Polymer 2004, 45, 8949.
7. Chirila, T. V.; Chen, Y. C.; Griffin, B. J.; Constable, I. J. Polym Int 1993, 32, 221.

8. Iizawa, T.; Taketa, H.; Maruta, M.; Ishido, T.; Gotoh, T.; Sakohara, S. J Appl Polym Sci 2007, 104, 842.
9. Shibayama, M.; Nagai, K. Macromolecules 1999, 32, 7461.
10. Pacios, I. E.; Horta, A.; Renamayor, C. S. Macromolecules 2004, 37, 4643.
11. Pastoriza, A.; Pacios, I. E.; Pierola, I. F. Polym Int 2005, 54, 1205.
12. Calvino-Casilda, V.; Lopez-Peinado, A. J.; Vaganova, E.; Yitzchaik, S.; Pacios, I. E.; Pierola, I. F. J Phys Chem B 2008, 112, 2809.
13. Dusek, K.; Prins, W. Adv Polym Sci 1969, 6, 1.
14. Xue, W.; Champ, S.; Huglin, M. B.; Jones, T. G. J. Eur Polym J 2004, 40, 703.
15. Bromberg, L.; Grosberg, A. Y.; Matsuo, E. S.; Suzuki, Y.; Tanaka, T. J Chem Phys 1997, 106, 2906.
16. Pacios, I. E.; Molina, M. J.; Gomez-Anton, M. R.; Pierola, I. F. J Appl Polym Sci 2007, 103, 263.
17. Pacios, I. E.; Pierola, I. F. Macromolecules 2006, 39, 4120.
18. Molina, M. J.; Gomez-Anton, M. R.; Pierola, I. F. Macromol Chem Phys 2002, 203, 2075.
19. Molina, M. J.; Gomez-Anton, M. R.; Pierola, I. F. J Polym Sci, Part B: Polym Phys 2004, 42, 2294.
20. Isik, B.; Dogantekin, B. J Appl Polym Sci 2005, 96, 1783.
21. Maeda, Y.; Yamamoto, H.; Ikeda, I. Langmuir 2001, 17, 6855.
22. Valencia, J.; Pierola, I. F. J Polym Sci Part B: Polym Phys 2007, 45, 1683.
23. Valencia, J.; Pierola, I. F. J Appl Polym Sci 2002, 83, 191.
24. Molina, M. J.; Gomez-Anton, M. R.; Pierola, I. F. J Phys Chem B 2007, 111, 12066.
25. Molina, M. J.; Gomez-Anton, M. R.; Rivas, B. L.; Maturana, H.; Pierola, I. F. J Appl Polym Sci 2001, 79, 1467.
26. Guo, Z.; Sautereau, H.; Kranbuehl, D. E. Macromolecules 2005, 38, 7992.
27. Alves, N. M.; Ribelles, J. L. G.; Mano, J. F. Polymer 2005, 46, 491.
28. DiMarzio, E. A. J Res Natl Bur Stand 1964, 68, 611.
29. Flory, P. J. Principles of Polymer Chemistry; Cornell University Press: Ithaca, NY, 1953.
30. Brannon-Peppas, L. In Studies in Polymer Science 8, Absorbent Polymer Technology; Brannon-Peppas, L.; Harland, R. S., Eds.; Elsevier: New York, 1990; 45–67.
31. Valentin, J. L.; Carretero-Gonzalez, J.; Mora-Barrantes, I.; Chasse, W.; Saalwachter, K. Macromolecules 2008, 41, 4717.
32. Horta, A.; Pastoriza, A. Eur Polym J 2005, 41, 2793.
33. Dusek, K.; Duskova-Smrckova, M. In Macromolecular Engineering. Precise Synthesis, Material Properties, Applications; Matyjaszeuski, K.; Gnanou, Y.; Leibler, L., Eds.; Wiley-VCH: New York, 2007; Vol. 3, Chapter 8.